Indian Journal of Chemistry
Vol. 63, June 2024, pp. 613-620
DOI: 10.56042/ijc.v63i6.9771

Determining the most relevant crystal structure to virtually identify type 1 inhibitors of c-Met: Part A

Khushboo Begwani & Urmila Joshi*

Department of Pharmaceutical Chemistry, Prin. K. M. Kundnani College of Pharmacy, Cuffe Parade, Colaba, Mumbai 400 005, India

E-mail: urmila.joshi1365@gmail.com

Received 21 March 2024; accepted (revised) 29 May 2024

c-Met is a receptor tyrosine kinase, which plays a crucial role in cell proliferation, migration and angiogenesis. Its dysregulation results in aberrant signalling, resulting in tumor growth and metastasis; an important target in cancer treatment. Multiple crystal structures are available from the protein data bank of c-Met bound to various inhibitors. Since the receptor tyrosine kinases are conformationally flexible receptors, each of these crystal structures represents a distinct conformation suited to accommodate the ligand. For the identification of new ligands as inhibitors of c-Met using computational methods, such a situation presents a challenge, as the use of some crystal structures for docking may result in the identification of false negatives. To address this issue, we have screened the available crystal structures of c-Met; bound to Type 1 inhibitors systematically to identify the most relevant crystal structure which can be used for docking. The procedure involved ascertaining the presence of Type 1 inhibitors in the crystal structure, self-docking to ensure the suitability of docking protocol, cross-docking to establish the ability of that crystal structure to accommodate chemically distinct ligands and followed by judging the ability of the top-ranked crystal structures to identify actives over decoys preferentially. The Enrichment Factors and other statistical parameters such as the number of outranking decoys, Robust Initial Enhancement, ROC, BEDROC and Diversity Enrichment Factor were also calculated and analysed. All the results pointed towards 3ZXZ outperforming in all the tests and thus can be used as the most appropriate crystal structure for virtual screening of Type 1 inhibitors of c-Met.

Keywords: Type 1 inhibitors of c-Met, Self-docking, Cross-docking, Enrichment parameters

Receptor tyrosine kinases (RTKs) are kinases involved in the phosphorylation of 2-amino-3-(4-hydroxyphenyl)propanoic acid residues of some important proteins of the cell cycle[1]. Phosphorylation has a crucial role in promoting cell proliferation, migration and angiogenesis[2]. c-Met is a receptor tyrosine kinase, that binds to natural bio-ligand, Hepatocyte Growth Factor (HGF) and controls multiple biological processes including cell proliferation, survival, motility and morphogenesis[3]. Dysregulation of c-Met activation results in aberrant signalling via c-Met, resulting in tumor growth and metastatic progression[4]. Thus, c-Met has emerged as a vital target in drug identification and inhibitors of c-Met are sought-after compounds in cancer treatment.

c-Met, like all other RTKs is a conformationally flexible receptor. It is known to exist in at least two different conformations, the active and inactive conformation[5]. In active conformation, it can bind to ATP and cause phosphorylation. The inactive conformation blocks the entry of ATP into the active site of the receptor. The transition from inactive to active conformation takes place via the DFG sequence present near the active site. Inactive conformation (DFG-out), here the phenylalanine of the DFG conserved sequence points towards the substrate binding site, thereby blocking the binding ATP into the active site[6]. During the transition from inactive to active conformation (DFG-in), flipping of the DFG motif occurs such that the phenylalanine now points away from the active site whereas aspartate points towards the active site. This allows ATP to fit into the active site. Inhibitors binding to the active conformation of c-Met are known as Type 1 inhibitors, whereas inhibitors bound to the inactive conformation of c-Met are called Type 2 inhibitors. The presence of a c-helix near the active site introduces another point of conformational flexibility. The c-helix can move towards or away from the active site, generating two more conformations, viz. c-helix-in and c-helix-out[7]. Different conformations of the receptor are associated with different areas and shapes available for binding of inhibitors.

Virtual Screening (VS) is an important and strategic tool for the discovery of lead compounds as inhibitors

of c-Met. VS is further categorised as Structure-Based Virtual Screening (SBVS) and Ligand-Based Virtual Screening (LBVS)[8]. LBVS does not require a three-dimensional (3D) structure of the receptor to be known. The 3D structure of the ligand is considered complementary to the receptor. This method requires less computational time than the SBVS, but its accuracy is limited by the selection of accurate bioactive conformation of the ligand[9], given the flexibility of the ligand. SBVS on the other hand, involves computing interactions of ligands with the protein[10]. The most commonly used 3D structure of the protein is the x-ray crystal co-crystallized with the cognate ligand. Computation of the interactions between the ligand and the protein is done using docking and scoring functions so that the ligand affinity in the active site can be ranked.

The conformational flexibility of the RTKs and the fact that kinases are known to accommodate chemically distinct ligands by altering the conformation to fit the ligands[11]; calls for a careful anticipation of crystal structures for elevating the docking and virtual screening strategies. The protein pose in the crystal structure is adapted to suit the ligands of the same chemical scaffold. The other chemical classes may not fit well in crystal. Thus, the choice of the crystal structure may introduce a bias in the SBVS. With the availability of multiple crystal structures, co-crystallized with chemically distinct ligands, two options can be used to deal with the problem of choice of crystal structure for docking[12], the first one being docking into all available crystal structures; thereby removing the bias. This method, however, is computationally intensive approach. The other method involves a systematic selection of crystal structures most appropriate for docking[13]. Such systematic selection has been reported for CDK-2 inhibitors[14,15], VEGFR-2 inhibitors[16], BACE1[17] inhibitors and many more. Such selection is also reported for c-Met inhibitors[18]. The study, however, takes into account a limited number of crystal structures of Type 1 inhibitors of c-Met and the elimination of crystal structures is based on RMSD values associated with self and cross-docking.

In an attempt to carry out virtual screening for the development of Type 1 inhibitors, binding to DFG-in or active conformation of c-Met, we came across forty-three crystal structures of c-Met bound to different Type 1 inhibitors. All these crystal structures were in DFG-in, c-helix out (DICO) conformation. Considering the abundance of crystal structures accessible for docking analysis, we decided to choose the most significant crystal structure which can be used in SBVS, in search of Type 1 inhibitors of c-Met.

Experimental Section

Fifty-six crystal structures of c-Met kinase-containing co-crystallized inhibitors were reported in the RCS Protein Data Bank (PDB). Our general workflow consisted of the classification of the crystal structures into active and inactive, with further classification based on the conformation of the c-helix. This was followed by the application of a series of filters to the crystal structures containing Type 1 inhibitors, including quality of the crystal structure, presence of missing residues in the substrate binding catalytic site, mutations, self-docking and cross-docking and finally application of statistical parameters to implement the most significant crystal structure for *in silico* studies.

Classification of the crystal structures using KLIF database[19]

The crystal structures were separated into active and inactive structures elicited by the binding on the DFG conformation. This method is based on comparing the distances of the three residues of the DFG motif and classifying them into active, inactive and intermediate. Accordingly, the bound inhibitors are Type-1, Type-2 and Type-1.5 inhibitors. Thus, finalised by selecting 43 crystal structures bound to Type 1 inhibitors.

Elimination of crystal structures based on resolution and R_{free} factor

The crystal structures with resolution greater than 2Å were eliminated from the study, to ensure that the quality of crystal structures is up to the mark. Similarly, structures with R_{free} factor greater than or equal to 0.26 were rejected.

Protein preparation

Twenty-eight crystal structures were imported into the workspace and prepared using the modules of the protein prep tab of Maestro ver. 11.011. Crystal structures have been prepared by assigning bond orders to all bonds in the structure, adding hydrogens to all atoms in the structure, and filling the skipped residues and loops. The water molecules were discarded beyond 5 Å, as no water bridge interactions

were reported. Missing hydrogen atoms were added to cognate ligands and subjected to ionization by PROPKA[20]. The structures were refined to relieve strain using imperf utility[21], and formal charges were added.

Receptor–grid generation

Grids were generated for docking ligands at the active site of the crystal with default settings adjusted at the receptor grid generation tab[22]. The centre coordinates of the co-crystallized ligand were selected to generate the centre of a grid box. The size of the grid created was 10 Å × 10 Å × 10 Å inner grid box. The Van Der Waals scaling and partial input charges were kept default.

Ligand preparation

The co-crystallized ligands of the aforementioned 28 crystal structures were prepared at pH 7.4 and performed minimization using OPLS-2005 ff using LigPrep program, Schrodinger MM share version 3.7.011 module[23]. In the preparation of ligands, the following steps were taken into consideration addition of hydrogen, ionization states, and tautomeric states and generalization of the 3D geometries. Performance indices and enrichment studies using standard precision mode in docking keeping other parameters set at default.

Protocol for self-docking and cross-docking

Each of the co-crystallized ligands was separated from each of the 28 crystal structures and prepared using Ligprep. Each cognate ligand was re-docked into its grid in crystal structure using the SP mode and 10 poses were generated from the Glide 6.7 module, Schrodinger suite. The cutoff specified for the scaling factor was set to 0.80, and the partial range cutoff was 0.15. The ligands giving Root Mean Square Deviation (RMSD) > 2 after self-docking were eliminated. This gave us 21 ligands and their cognate crystal structures.

Cross-docking protocol

The twenty-one ligands, selected after the self-docking step, were docked into twenty noncognate crystal structures during cross-docking. The mode selected for docking was SP. The docked pose of each ligand was superimposed on the native pose to calculate RMSD average RMSD was calculated by repeating this procedure for all the 10 saved poses. Analysis of average RMSD gave us ten top structures, which were subjected to decoy set validation.

Validation on decoy set

The next step involved the selection of 100 Type 1 c-Met inhibitors reported in the literature, with IC_{50} values of 0.1 μM–10 μM belonging to diverse chemical classes[24–27]. The chemical classes of Type 1 c-Met inhibitors included in this study belonged to triazolopyrazinyl quinolines, quinolines, triazolothiadiazoles, benzoxazoles, quinoxalines, spiro[indoline-3,4'-piperidine]-2-ones, indazoles, pyridazinonequinoline, 2,4-diaminopyrimidine substituted at 5,5-dimethylbenzazepinone, benzazepinone imidazo[1,2-a]pyridines, 6-aminofuro[3,2-c]pyridine and benzothiazole. The decoy molecules were selected specifically for c-Met kinase from the DUD-E database[28]. The 4336 decoy molecules were imported from the DUD-E website at the Maestro interface. All the actives as well as decoy molecules were generated using LigPrep by examining the lowest-energy ionization and tautomeric states at pH of 7.4. The scaling factor was fixed at 0.80, and the partial charge cutoff was set to 0.15. We selected the option to retain the chiralities of the molecules, and the energy was minimized using the OPLS 2005 force field.

Enrichment factor calculation

We calculated Enrichment Factors (EF1% and EF2%)[29], ROC-AUC[30], Robust Initial Enhancement (RIE)[31], BEDROC[32] as well as Diversity-based Enrichment Factor (DEF)[32] from the docking results of the actives and decoys.

The diversity-based enrichment factor (DEF), measures the impact on enrichment scores when there's low structural variety among compounds. DEF is calculated by multiplying EF by the ratio of diversity among the retrieved active compounds to the maximum diversity within the entire set of active compounds. The determination of similarity is done by the following equation in decoy set screening:

$$DEF = EF \times \frac{1-\min(Sim_{Hits})}{1-\min(Sim_{Actives})} \text{ equation} \quad \ldots (1)$$

Results and Discussion

Classification of the crystal structures using KLIF database

Conformation of kinase in active and inactive states varies to a great extent and therefore does the size and the shape of the ligand-binding pocket of that kinase. This calls for ascertaining the conformation of the kinase before carrying out docking studies. The DFG conformation is very crucial in deciding the state of kinase. Conformation of the c-helix was an

Table 1 — Resolution and R_{free} factor of Type-I crystal structures

Sr. No.	PDB	Resolution	Free Rfac	Sr. No.	PDB	Resolution	Free Rfac
1	2RFS	**2.2	0.26	23	4XMO	1.75	0.24
2	2WD1	2	#0.27	24	4XYF	1.85	0.24
3	2WGJ	2	0.23	25	5EOB	1.75	0.2
4	2WKM	**2.2	0.28	26	5EYC	1.8	0.25
5	3CD8	2	#0.29	27	5EYD	1.85	0.25
6	3F66	1.4	0.23	28	5HNIX	1.71	0.24
7	3I5N	2	#0.27	29	5HOA	**2.14	-
8	3ZBX	**2.2	0.24	30	5UAB	1.9	0.23
9	3ZC5	**2.2	0.26	31	5UAD	**2.25	0.25
10	3ZCL	1.4	0.21	32	5YA5	1.89	0.23
11	3ZXZ	1.8	0.22	33	6SDE	**2.49	0.27
12	3ZZE	1.87	0.23	34	6UBW	2	0.23
13	4AOI	1.9	0.21	35	7B3Q	1.75	0.19
14	4AP7	1.8	0.21	36	7B3T	**2.23	0.26
15	4DEG	2	0.25	37	7B3V	1.93	0.25
16	4DEH	2	0.26	38	7B3Z	1.8	0.21
17	4DEI	**2.05	0.29	39	7B40	1.76	0.23
18	4GG5	**2.42	0.27	40	7B41	1.97	0.23
19	4GG7	**2.27	0.26	41	7B42	1.8	0.23
20	4KNB	**2.4	0.29	42	7B43	1.87	0.23
21	4R1V	1.2	0.18	43	7B44	1.76	0.25
22	4R1Y	2	0.24	–	–	–	–

Where ** and # indicate the crystal excluded in resolution and R_{free} factor

additional factor taken into consideration. The active state of kinase is identified by the distances of the amino acids of the DFG-motif. KLIF database was used to filter the DFG-in, c-helix-out conformations. This gave us 43 crystal structures to start with.

Elimination of crystal structures based on resolution and R-$_{free}$ factor

Table 1 shows the details of crystal structures eliminated based on resolution and R_{free} factor.

For any protein structure, resolution values of around 1Å are considered excellent and every atom can be seen in the electron density map. However, there are very few structures with such resolution. Lower-resolution structures, with a resolution of about 3Å, may not represent the atomic structure correctly. After taking this literature report into consideration, coupled with the fact that there are hardly any structures with a resolution less than or equal to 1Å deposited in the protein data bank, we decided to strike a balance and eliminate crystal structures with a resolution greater than 2Å from the study[34]. This resulted in the survival of 31 crystal structures from among a total of 43 crystal structures.

R_{free} factor relates the amplitudes of observed and calculated reflection of the crystal. This gives unbiased refinement of the crystal. Although the ideal value is nearer to zero, the value of 0.20 is considered to be an excellent value. The value above 0.26 is considered to be associated with a less accurate crystal[35]. This prompted us to eliminate crystal structures with values greater than 0.26. This resulted in the elimination of three crystal structures, viz 2WD1, 3CD8 and 3I5N. We were left with 28 crystal structures satisfying the filtration criteria.

Table 2 — Average RMSD values of self-docking

Crystal	RMSD	Crystal	RMSD	Crystal	RMSD	Crystal	RMSD
2WGJ	1.79	4DEG*	2.23	5EYC*	2.03	7B3V	1.58
3F66	0.99	4DEH	1.86	5EYD*	2.06	7B3Z	1.52
3ZCL*	2.78	4R1V*	2.46	5HNI*	2.20	7B40	1.54
3ZXZ	1.07	4R1Y*	2.24	5UAB	1.49	7B41	1.47
3ZZE	1.67	4XMO*	2.81	5YA5	1.69	7B42	1.81
4AOI	1.52	4XYF	1.62	6UBW*	2.23	7B43	1.31
4AP7	0.93	5EOB	1.47	7B3Q	1.43	7B44	0.59

* Indicates crystal structure in which the average RMSD value is above 2Å in self-docking

Self-docking and cross-docking

RMSD between a docked conformation and the co-crystallized ligand gives the pose with the accepted criterion for assessing the accuracy of docking[36]. 19 of 28 native ligands had an RMSD <2Å in the self-docking experiment in Table 2.

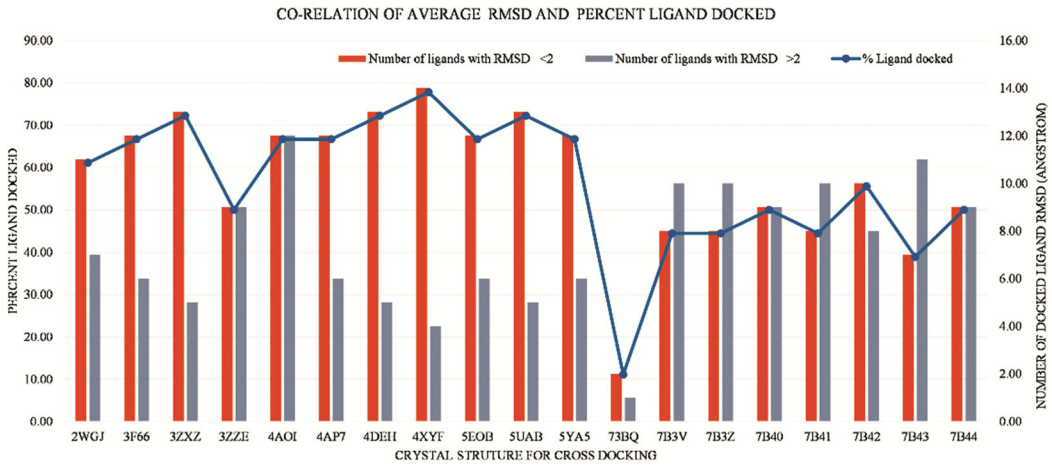

Fig. 1 — Percent ligand docked and the number of RMSD of docked ligands with <2 and >2 crossed in 19 pdbs

Crystal structures that fit the non-cognate ligands show the lowest RMSD postulated to perform better in virtual screening experiments[37]. Non-native ligands were docked into different crystal structures and RMSD value was calculated for the docked pose with the native pose.

Fig. 1 depicts the percentage of noncognate ligands docked in each crystal structure, the number of ligands with RMSD >2Å as well as <2Å in the cross-docking experiment. Crystal structure with PDB ID 4XYF docked nearly 80% of ligands, whereas crystal structure with PDB ID 73BQ docked only 10% of ligands.

In terms of the number of ligands docked with RMSD <2Å, 4XYF docked 14 ligands while 73BQ docked only 2. Other crystal structures that docked ligands a greater number of ligands with RMSD <2Å included 4DEH, 5UAB, 5YA5, 3ZXZ, 3F66, 5EOB, 4AP7, and 7B42. Some crystal structures docked an equal number of ligands with RMSD <2Å and >2Å. These included 4AOI, 7B44, and 3ZZE. Lastly, crystal structures docking a greater number of ligands with RMSD >2Å included 7B3V, 7B3Z, 7B41, and 7B43.

Enrichment factor

Enrichment analyses offer valuable perspectives on the role of effective screening of the crystal. These metrics measure the active compounds relative to the inactive ones in the top screened list[22,31]. The performance of virtual screening is related to the capacity to prioritize active molecules in the early screening phase, given that typically the initial segment of the virtual entries undergoes experimental screening.

Table 3 — Enrichment factor calculation at various percentages

DB	1%	2%	5%	10%	20%
2WGJ	41	25	12	7.1	4.1
3F66	41	24	13	7.3	4.1
3ZXZ	53	39	18	9.1	4.6
4AOI	45	26	13	7.3	3.9
4AP7	29	20	9.6	5.8	3.7
4DEH	34	23	12	6.4	4
4XYF	38	23	12	6.7	3.6
5EOB	41	25	13	7.5	3.9
5UAB	39	24	13	7.5	3.9
5YA5	45	28	13	7.3	4.2

During the enrichment studies, the initial parameter assessed was the enrichment factor at various percentages (1%, 2%, 5%, 10%, and 20%) of the ranked dataset. The enrichment factor values for PDB structures are provided in Table 3. Only one crystal structure displayed an EF1% greater than 50 while other crystals had less than 50.

Receiver operating characteristic (ROC) curves

ROC curves facilitate a graphical assessment of how effectively crystal structures can differentiate between active compounds and decoys, represented by pairs of sensitivity and specificity[32]. The perfect curve achieves full sensitivity that extends diagonally, and all active compounds and decoys are correctly identified, resulting in sensitivity = 1 and specificity = 0. On the contrary, when examining the curve for a particular collection of actives and decoys when scores are at random, it converges asymptotically towards the line Se = 1 – Sp when total actives and decoys are screened and signify randomness by manifesting a diagonal pattern (Fig. 2). All assessed crystal structures in the investigation demonstrated

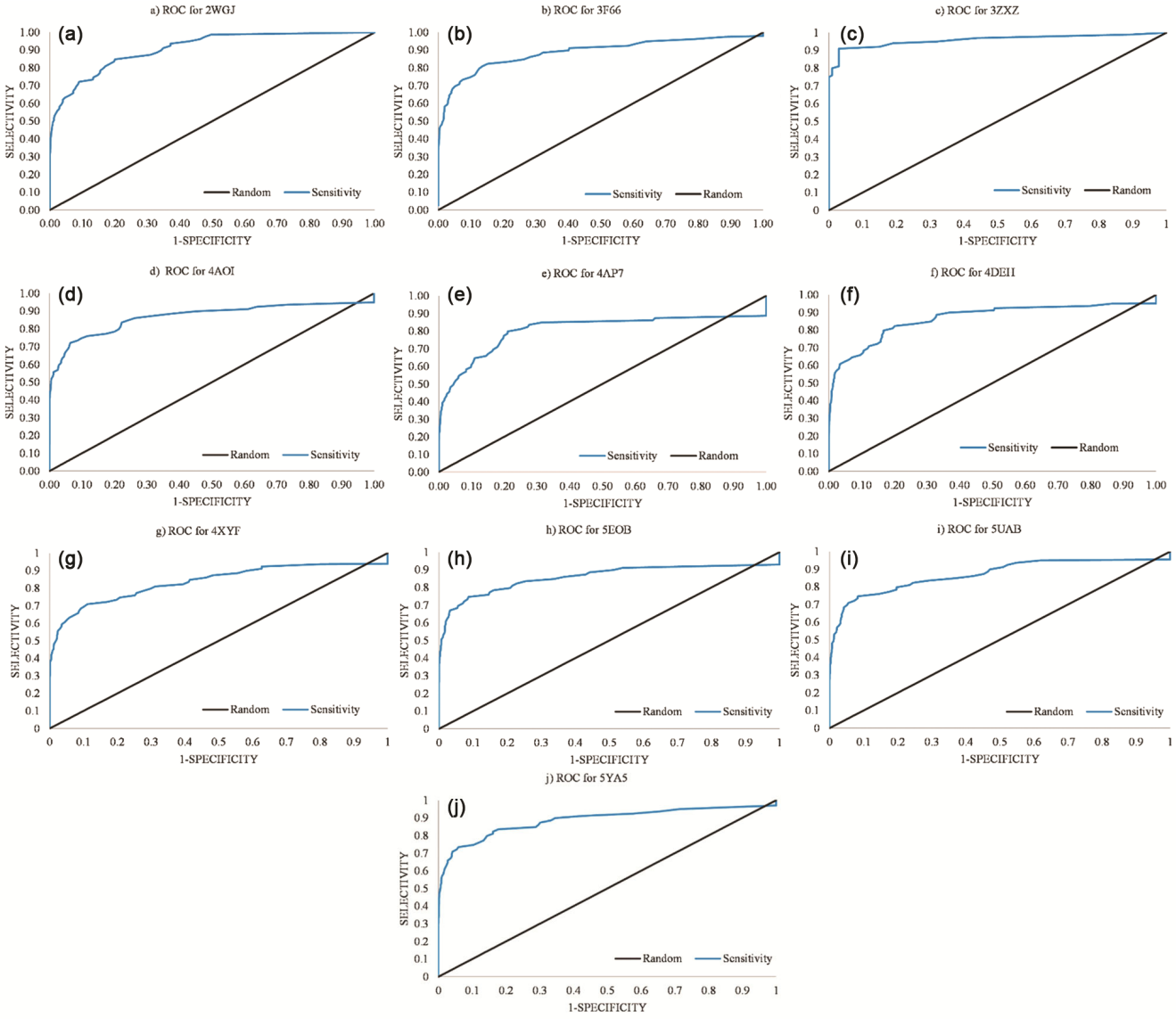

Fig. 2 — Representation of a-j ROC of ten crystal

performance superior to random screening. The pdb 2WGJ and 3ZXZ both displayed maximum ROC values of 0.91 and 0.95 respectively. The ROC curves are given below.

Area under the curve (AUC)

Fig. 3 shows the results obtained for AUC and Numbering. of Outranking Decoys for the ten crystal structures that underwent further analysis.

The AUC serves as a numerical measure of performance and facilitates quantitative comparison. A commonly accepted guideline for assessing screening accuracy[31] is as follows: AUC values between 0.90 and 1 indicate excellent performance, in contrast, ones falling within the range of 0.80 and

Fig. 3 — Co-relation of AUC and numbering of outranking decoys

0.90 are considered acceptable. AUC values ranging from 0.70 to less than 0.8 are deemed fair, while those between 0.50 and less than 0.70 are considered poor. AUC values below 0.50 represent failure. All crystal structures had good to excellent AUC values with 3ZXZ having the highest AUC value.

Average number of outranking decoys

The total account of decoys outranks the actives is determined by subtracting one from the adjusted rank of each active. This process is repeated for all docked actives, and the average number of outranked decoys is computed[15]. PDB 3ZXZ has the lowest number of outranking decoys while 4XYF has the highest number of outranking decoys.

All the above-mentioned results point towards 3ZXZ being the crystal structure of choice. However, the parameters discussed so far are the classical parameters. These parameters fail to differentiate between highly ranked active molecules and those ranked lower in a list[15]. Consequently, if two crystal structures exhibit differing abilities in the rank list to prioritize the high-scoring active molecules initially but demonstrate a similar degree of enrichment for active molecules, considered equally effective. Hence, it was imperative to evaluate and compare them based on advanced enrichment parameters.

Robust initial enhancement (RIE)

RIE act as a sophisticated metric for enrichment, quantifying the ranking process of a crystal that outperforms the selection of actives. RIE with the above indicates surpassing the randomness. Remarkably, every crystal structure demonstrated RIE exceeding 1, thereby emphasizing their superior performance over random.

The Boltzmann enhanced discrimination of ROC (BEDROC)

The Boltzmann enhanced discrimination of ROC (BEDROC) works as the measuring parameter correlates with the α-value and later represents the portion of the total score at a specific percentile of the ranked list. For instance, an α-value set at 20 suggests that 8% accounts for 80% of the total contribution, emphasizing early recognition[31]. When maintaining the maximum contribution at 80%, an α-value is 20 indicates the arising from 8% of the list. During the examination of the two crystals, a crucial cutoff is αRa<< 1. These values are given in Table 4. The crystal 3ZXZ gained 0.86 at BEDROC α=20, whereas other crystal structures scored 0.61–0.69. While the crystal 4AP7 had the lowest 0.51. Correlating BEDROC α=20 with the ROC and RIE 3ZXZ had high values 0.95 and 14.51 respectively. Simultaneously, crystal 4AP7 showed the lowest values of ROC and RIE 0.80 and 8.65.

Table 4 — Advanced enrichment parameters

Crystal	ROC	RIE	BEDROC (α= 20.0)
2WGJ	0.91	10.56	0.63
3F66	0.88	11.05	0.66
3ZXZ	0.95	14.51	0.86
4AOI	0.86	11.08	0.66
4AP7	0.80	8.65	0.51
4DEH	0.86	10.16	0.60
4XYF	0.83	10.15	0.60
5EOB	0.85	11.17	0.66
5UAB	0.86	10.87	0.65
5YA5	0.88	11.56	0.69

Table 5 — DEF value at various % fractions of out-performed including active ligands and decoys

Crystal	DEF 1%	DEF 2%	DEF 5%	DEF 10%	DEF 20%
2WGJ	41	25	12	7.1	4.1
3F66	41	24	13	7.3	4.1
3ZXZ	53	39	18	9.1	4.6
4AOI	44	26	13	7.3	3.9
4AP7	29	19	9.6	5.8	3.7
4DEH	34	23	12	6.4	4
4XYF	38	23	12	6.7	3.6
5EOB	41	25	13	7.4	3.9
5UAB	39	24	13	7.4	3.9
5YA5	45	28	13	7.3	4.2

Diversity-based enrichment factor DEF

DEF prioritizes retrieving a combination of numerous and diverse active compounds concurrently, suggesting that discovering two highly dissimilar compounds may yield superior results compared to identifying ten nearly identical ones. DEF may enhance the chances of discovering novel and effective compounds by considering a broader range of chemical structures and properties[33]. The DEF observed at different % mentioned in Table 5.

Conclusion

Detailed research was initiated to ascertain the crystal structure of c-Met; co-crystallized with Type 1 inhibitors, which can accommodate chemically diverse ligands and is thus best suited for virtual screening using docking. All the selected crystal structures were in DFG-in, c-helix out conformation. After a detailed study of self and cross-docking and calculation of enrichment parameters we conclude that from among

the crystal structures included in the present study, 3ZXZ is the most relevant structure for conducting the virtual screening, involving docking studies to gain insight into the development to target the c-Met.

Supplementary Information

Supplementary information is available on the website http://nopr.niscpr.res.in/handle/123456789/58776.

Acknowledgement

The authors acknowledge the facility under DST-SERB File No. EMR/2017/000250 (vide Diary No. SERB/F/7466/2018-2019 dated 25th September 2018).

References

1 Mouna C, Ahmed R, *J Recept Signal Transduct Res*, 31 (6) (2011) 387.
2 Ahsan R, Khan, M. M, Mishra, A, Noor G & Ahmad U, *J Protein Chem*, 42 (6) (2023) 621.
3 Raj S, Kesari K K, Kumar A, Rathi B, Sharma A, Gupta P K, Jha S K, Jha N K, Slama P, Roychoudhury S & Kumar D, *Mol Cancer*, 21 (1) (2022) 1.
4 Wang H, Rao, B, Lou J, Li J, Liu Z, Li A, Cui G, Ren Z & Yu Z, *Front Cell Dev Biol*, 8 (2020) 1.
5 Uchikawa E, Chen Z, Xiao G Y, Zhang X & Bai X Chen, *Nat Commun*, 12 (1) (2021) 1.
6 Vijayan R S K, He P, Modi V, Duong-Ly K C, Ma H, Peterson J R, Dunbrack R L & Levy R M, *J Med Chem*, 58 (1) (2015) 466.
7 Jiang T, Liu Z, Liu, W, Chen J, Zheng Z & Duan M, *J Chem Inf Model*, 62 (15) (2022) 3651.
8 Li J, Liu, W, Song Y & Xia J, *RSC Adv*, 10 (13) (2020) 7609.
9 Sabe V T, Ntombela, T, Jhamba L A, Maguire G E M, Govender T, Naicker T & Kruger H G, *Eur J Med Chem*, 224 (2021) 1.
10 Qin T, Zhu Z, Wang X S, Xia J & Wu S, *Expert Opin Drug Dev*, 16 (10) (2021) 1175.
11 Meng Y, Pond M P & Roux B, *Acc Chem Res*, 50 (5) (2017) 1193.
12 Cheng T, Li Q, Zhou Z, Wang Y & Bryant S H, *AAPS J*, 14 (1) (2012) 133.
13 Chandan R, Chaithanya M S, Aditya M & Kiran K S, *J Biomol Struct Dyn*, 41 (17) (2023) 8383.
14 Sperandio O, Mouawad L, Pinto E, Villoutreix B O, Perahia D & Miteva M, *Eur Biophys J*, 39 (9) (2010) 1365.
15 Bhojwani H R & Joshi U J, *Curr Comput-Aided Drug Des*, 13 (3) (2017) 186.
16 Mateev E, Valkova I, Georgieva M & Zlatkov A, *Int J Pharm Sci Res*, 13 (3) (2022) 1099.
17 Haghighijoo Z, Hemmateenejad B, Edraki N, Miri R & Emami S, *J Mol Graph*, 76 (2017)128.
18 Yuan H, Liu Q, Zhang L, Hu S, Chen T, Li H, Chen Y, Xu Y & Lu T, *Eur J Med Chem*, 143 (2018) 491.
19 Van Linden O P J, Kooistra A J, Leurs R, De Esch I J P & De Graaf C, *J Med Chem*, 57 (2) (2014) 249.
20 Olsson M H M, Søndergaard C R, Rostkowski M & Jensen J H, *J Chem Theory Comput*, 7 (2) (2011) 525.
21 Schrodinger, LLC, New York, NY.
22 Halgren T A, Murphy R B, Friesner R A, Beard H S, Frye L L, Pollard W T & Banks J L, *J Med Chem*, 47 (7) (2004) 1750.
23 Wan H, Selvaggio G & Pearlstein, R. A, *PLOS ONE*, 15 (11) (2020) 1.
24 Parikh P K & Ghate M D, *Eur J Med Chem*, 143 (2018) 1103.
25 Wang Y, Ai J, Wang Y, Chen Y, Wang L, Liu G, Geng M & Zhang A, *J Med Chem*, 54 (7) (2011) 2127.
26 Zhao F, Zhang L D, Hao Y, Chen N, Bai R, Wang Y J, Zhang C C, Li G S, Hao L J, Shi C, Zhang J, Mao Y, Fan Y, Xia G X, Yu J X & Liu Y J, *Eur J Med Chem*, 134 (2017) 147.
27 Ye L, Ou X, Tian Y, Yu B, Luo Y, Feng B, Lin H, Zhang J & Wu S, *Eur J Med Chem*, 65 (2013) 112.
28 https://dude.docking.org/
29 Feinstein W P & Brylinski M, *J Cheminform*, 7 (1) (2015) 7.
30 Torres P H M, Sodero A C R, Jofily P & Silva-Jr F, *Int J Mol Sci*, 20 (18) (2019) 1.
31 Truchon J F, Bayly C I, *J Chem Inf Model*, 2 (2007) 488.
32 Salam N K, Nuti R & Sherman W, *J Chem Inf Model*, 49 (10) (2009) 2356.
33 Reddy K K, Singh S K, *Chem-Biol Interact*, 218 (2014) 71.
34 Wang J, *Protein Sci*, 24 (5) (2015) 661.
35 Brunger A T, *Nature*, 355 (1992) 472.
36 Cross J B, Thompson D C, Rai B K, Baber J C, Fan K Y, Hu Y & Humblet C, *J Chem Inf Model*, 49 (6) (2009) 1455.
37 Chen X, Liu H, Xie W, Yang Y, Wang Y, Fan Y, Hua Y, Zhu L, Zhao J, Lu T, Chen Y & Zhang Y, *J Chem Inf Model*, 59 (12) (2019) 5244.
38 Qaoud M & Şüküroğlu M, *Pal Med Pharm J*, 3 (2023) 343.